



## EXTRACTING ELECTRICAL PARAMETERS OF SOLAR CELLS USING LAMBERT FUNCTION

Mohammed BOUZIDI <sup>1,2,\*</sup> , Mohamed Ben Rahmoune <sup>1,3</sup> , Abdelfatah NASRI <sup>4</sup> ,  
Smail MANSOURI <sup>5</sup> , Messaoud HAMOUDA <sup>6</sup> 

<sup>1</sup> Department of Sciences and Technology, Faculty of Sciences and Technology, University of Tamanrasset, Algeria

<sup>2</sup> Energy and Materials Laboratory, University of Tamanghasset, Algeria.

<sup>3</sup> Applied Automation and Industrial Diagnostics Laboratory, Faculty of Science and Technology, University of Djelfa 17000 DZ, Algeria

<sup>4</sup> Laboratory Smart Grid and Renewable Energy SGRE University Tahri Mohamed Bechar Algeria

<sup>5</sup> Faculty of Sciences and Technology, University of Ahmed Draia, Adrar, Algeria

<sup>6</sup> Department of Energy Technology, DDI Laboratory, Ahmed Draia University, 01000 Adrar, Algeria

\* Corresponding author, e-mail: [mohbouzidi81@yahoo.fr](mailto:mohbouzidi81@yahoo.fr)

### Abstract

Photovoltaic cells are intricate systems that transform solar energy into electrical power. Certain internal parameters, such as diode saturation current, conversion resistance, and series resistance, significantly influence the performance of electrical components. Frequently, manufacturers do not provide these parameters. At the moment, researchers need new and clear ways to measure these factors so they can get a better idea of how solar cells work and improve efficiency through simulations. We present a novel approach to accurately determining the five parameters (series resistance, shunt resistance, photovoltaic cell current, and diode saturation current) for multi-crystalline silicon solar cell models. This approach employs the Lambert function and the curve of parasitic resistance. By utilizing the extracted internal electrical parameters, this method will enhance the efficiency of solar cells through the facilitation of more accurate simulations.

Keywords: extraction of parameters, photovoltaic cells, function Lambert W, factor of ideality, single diode

## 1. INTRODUCTION

The utilization of solar energy technology has significant potential as an ecologically sound solution for attaining sustainability. Photovoltaic solar power is a widely used type of sustainable energy. The process entails the transformation of sunlight into electricity through the utilization of the photovoltaic effect. The current-voltage (I-V) curve illustrates the unique characteristics and effectiveness of a solar cell. Photovoltaic utilize the vast energy of the sun to produce environmentally friendly electricity [1-4].

The current-voltage (I-V) characteristic provides valuable insights into how a solar cell responds to variations in applied voltage and current. Analyzing the I-V curve is essential for evaluating the electrical efficiency of the cell and determining its capacity to convert sunlight into electrical energy [3-4].

The (I-V) curve illustrates the correlation between the current (I) and voltage (V) of the cell, given specific test conditions. The process enables the retrieval of crucial parameters such as open-

circuit voltage (Voc), short-circuit current (Isc), maximum power point, fill factor, and efficiency. An analysis of the curve's shape and characteristics can yield insights into shunt and series resistances, ideality factors, and other phenomena. In general, the I-V characteristic is a fundamental component used to analyze and enhance the performance of photovoltaic devices. The data obtained from the curve assists researchers in identifying constraints on performance and potential areas for enhancing the power output and conversion efficiency of the solar cell through design improvements [2-3].

This graph makes it easier to find out important things about cells, like their maximum power point, best operating points, conversion efficiency, open-circuit voltage (Voc), and short-circuit current (Isc) [5-6]. Possible constraints of the technology employed in the fabrication of solar cells may encompass deficiencies in the cell structure or the manufacturing processes. These imperfections may consist of material impurities, unregulated production processes, and other factors that can hinder the performance of solar cells. To evaluate

these imperfections and enhance the quality of solar cells, a thorough analysis of their electrical attributes using the I-V characteristic is essential.

The research emphasis has shifted towards solar cell modelling due to the growing utilization of solar systems. A significant number of studies employ the single-diode model, which relies on variables such as short-circuit current and diode saturation current. Precise models are essential for the design and optimization of photovoltaic systems [6–8].

Precisely determining the parameters of solar cell models continues to be difficult, yet it is crucial for simulation, quality assurance, and manufacturing purposes. The Shockley equation's implicit current function necessitates the simultaneous consideration of multiple variables. The Lambert W function facilitates the derivation of analytical solutions for obtaining these parameters [9–12].

This paper introduces a novel method for precisely determining the crucial electrical characteristics of solar panels. The method employs graphical representation and the Lambert function to approximate parameter values. The analysis enhances comprehension of solar panel performance and optimizes the utilization of solar energy.

## 2. THE PROPOSED METHODOLOGY

This study presents a newly devised technique to overcome the barriers that impede the successful extraction of electrical information from solar cells. The study is structured into two main phases to comprehensively examine the electrical performance of these cells from all angles.

The initial stage of the study involved utilizing the Lambert function to compute electrical parameters. This was done by employing various estimated values for the diode ideality factor ( $n$ ), which encompassed a spectrum of values ranging from 1 to 1.6. The objective of this section is to examine the impact of altering the value of  $n$  on the efficiency of the photovoltaic cell.

In the second step of the process, the model's series resistance ( $R_s$ ) and shunt resistance ( $R_{sh}$ ) were looked at to get the most accurate estimate of the diode ideality factor.

The objective of this section is to improve the precision of estimating the ideality factor by utilizing existing data instead of depending on prior estimations.

The experimentation was conducted on an MSX-77 polycrystalline silicon solar panel, comprising 36 photovoltaic cells. Table 1 presents the electrical data of a solar panel when subjected to Standard Test Conditions (STC), with a temperature of 25° and an irradiance of 1000 W/m<sup>2</sup>. This confirms the validity of the suggested method for enhancing the estimation of electrical parameters in a panel.

Table 1. The data sheet from the manufacturer (Typical Electrical Parameters)

Maximum power	77W (0/+5 W)
MPP voltage ( $V_{mp}$ )	16.9V
MPP Current ( $I_{mp}$ )	4.56A
Open circuit voltage ( $V_{oc}$ )	21V
Short circuit current ( $I_{sc}$ )	5A
Number of photocells	36

## 3. MODELLING OF PHOTOVOLTAIC SYSTEMS

The solar cell's mathematical model is derived from the PN junction model. Furthermore, we include the photocurrent, represented as  $I_{ph}$ , which is directly proportional to the intensity of irradiation.

Additionally, we propose the introduction of a term to govern internal electrical processes. Figure 1 displays the electrical circuit that corresponds to a solar cell containing a single diode. While  $V_T$  refers to the thermal voltage of the diode,  $I_{ph}$  stands for the current that the photovoltaic cell produces. Equations (1) and (2) demonstrate the correlation between these two numerical values.

Several scholars have extensively examined this topic in their publications [7–8] and [13–18].

$$I = I_{ph} - I_0 \left[ \exp \left( \frac{V + IR_s}{nV_T} \right) - 1 \right] - \frac{V + IR_s I}{R_{sh}} \quad (1)$$

$$V_T = N_s \frac{KT}{q} \quad (2)$$

Where  $n$  represents the ideality factor of the diode,  $R_s$  represents the series resistance, and  $R_{sh}$  represents the shunt resistance, in addition to:  $K$  represents Boltzmann's constant, which has a value of  $1.38006 \times 10^{-23} \text{J/K}$ .  $T$  denotes the temperature of the cell, measured in degrees Kelvin (°K).  $q$  Symbolizes the electric charge, with a value of  $1.60218 \times 10^{-19} \text{C}$ .

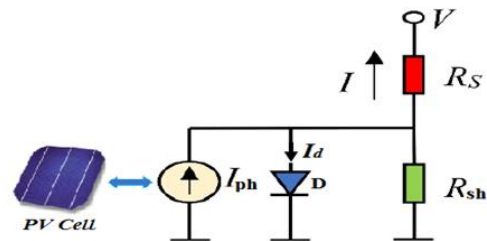


Fig.1. Solar cell model with a single diode

It can be seen in the figures (2), (3), and (4) how the ideality factor ( $n$ ), series resistance ( $R_s$ ), and shunt resistance ( $R_{sh}$ ) change the current-voltage (I-V) relationship. An analysis of the presented curves reveals that series resistance ( $R_s$ ) causes a decrease in the current in a solar cell, while parallel resistance ( $R_{sh}$ ) leads to an increase in shunt current and a decrease in cell current. The ideality factor has an impact on cell current, depending on the extent to which it deviates from ideal behavior.

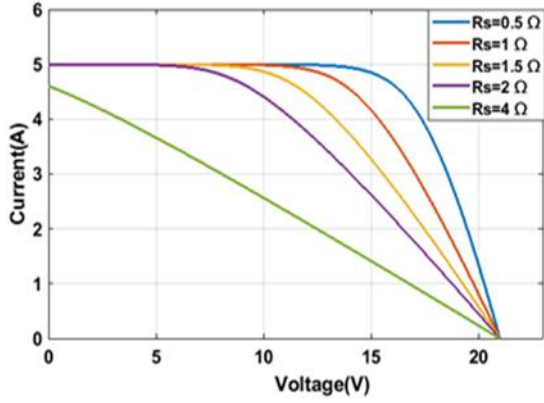


Fig. 2. The effect of series resistance on (I-V) characteristics.

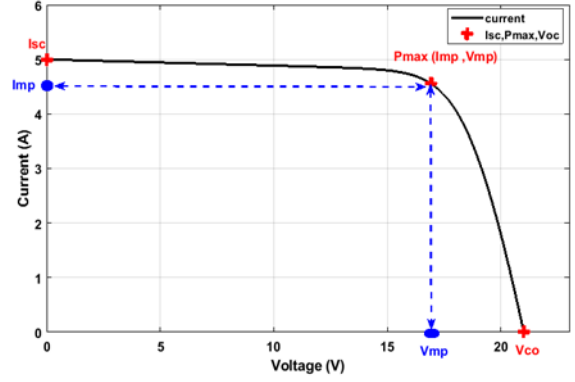


Fig. 5. (IV) characteristics of photovoltaic modules

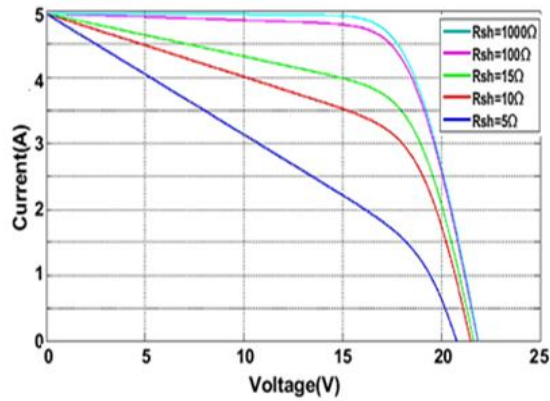


Fig. 3. The effect of parallel resistance on (I-V) Characteristics

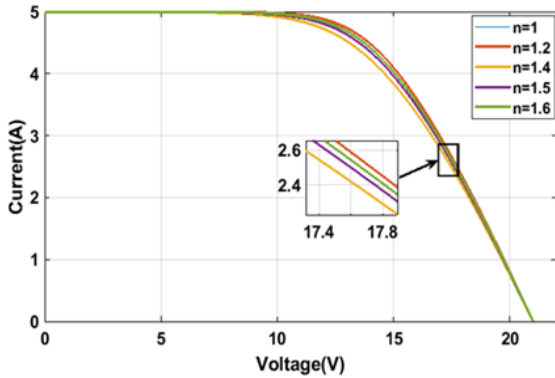


Fig. 4. The impact of the diode ideality factor on the photovoltaic cell's characteristic (I-V)

#### 4. DETERMINE PV PANEL MODEL PARAMETERS

To determine the five fundamental parameters of the photovoltaic panel, we will examine the I (V) characteristic curve at three distinct operating points. The short-circuit point; the maximum power point, and the open-circuit point are the three key points. As shown in Figure 5.

Equations (1) [7], [19–21] represent the three key points of I(V) characteristics:

$$I_{sc} = I_{ph} - I_0 \left[ \exp \left( \frac{I_{sc} R_s}{n V_T} \right) - 1 \right] - \frac{I_{sc} R_s}{R_{sh}} \quad (3)$$

$$I_{oc} = 0 = I_{ph} - I_0 \left[ \exp \left( \frac{I_{sc} R_s}{n V_T} \right) - 1 \right] - \frac{V_{oc}}{R_{sh}} \quad (4)$$

$$I_{mp} = I_{ph} - I_0 \left[ \exp \left( \frac{V_{mp} + I_{mp} R_s}{n V_T} \right) - 1 \right] - \frac{V_{mp} + I_{mp} R_s}{R_{sh}} \quad (5)$$

At the inflection point, the maximum power produced by a panel is zero when the derivative of power with respect to voltage is zero, which is the product of the maximum current ( $I_{mp}$ ) and the maximum voltage ( $V_{mp}$ ) [7], [19–20].

$$\frac{\partial P}{\partial V} = 0 = \frac{\partial (V \cdot I)}{\partial V} = V \frac{\partial I}{\partial V} + I = 0 \quad (6)$$

$$\left. \frac{\partial I}{\partial V} \right|_{I_{mp}, V_{mp}} = - \frac{I_{mp}}{V_{mp}} \quad (7)$$

The value of the limit between the brackets in equation (3) on the right-hand side is negligible compared to the other side [7-9], [20-21]:

$$I_{ph} = \left( \frac{R_s + R_{sh}}{R_{sh}} \right) I_{sc} \quad (8)$$

References [21–22] describe how to deduce the relationship for the current  $I_0$  using Equation (4):

$$I_0 = \left( I_{sc} - \frac{V_{oc} - I_{sc} R_s}{R_{sh}} \right) e^{-\frac{V_{oc}}{n V_T}} \quad (9)$$

Mr. A and others in [7], [21–24], and Dezsó S and others in [25] examined Equations (10), (11), and (12).

$$I_{mp} = I_{sc} - \left( I_{sc} - \frac{V_{oc} - R_s I_{sc}}{R_{sh}} \right) e^{\left( \frac{V_{mp} + I_{mp} R_s - V_{oc}}{n V_T} \right)} - \frac{V_{mp} + I_{mp} R_s - R_s I_{sc}}{R_{sh}} \quad (10)$$

$$e^{\left( \frac{V_{mp} + I_{mp} R_s - V_{oc}}{n V_T} \right)} = \frac{n V_T V_{mp} (2 I_{mp} - I_{sc})}{(V_{mp} I_{sc} + V_{oc} (I_{mp} - I_{sc})) (V_{mp} - I_{mp} R_s) - n V_T (V_{mp} I_{sc} - V_{oc} I_{mp})} \quad (11)$$

$$\frac{1}{R_{sh}} \Big|_{I=I_{sc}} = \frac{\frac{(I_{sc}R_{sh}-V_{oc}+I_{sc}R_s)\exp\left[\frac{I_{sc}R_s-V_{oc}}{nV_T}\right]}{nV_T R_{sh}}}{1 + \frac{(I_{sc}R_{sh}-V_{oc}+I_{sc}R_s)\exp\left[\frac{I_{sc}R_s-V_{oc}}{nV_T}\right]}{nV_T R_{sh}} + \frac{R_s}{R_{sh}}}$$

(12)

To determine the series resistance ( $R_s$ ) of the equivalent circuit [7], [20–25], transform equation (11) into an explicit equation using the Lambert ( $w$ ) function.

$W(y)$  represents the Lambert  $W$  function, which is the mathematical inverse of itself. It solves equations of the form [22–28].

$$Y = Xe^X \quad (13)$$

Then the Lambert  $W$  function,  $W(y)$ , is the function that allows you to find  $x$  in terms of  $y$ :

$$x = W(y) \quad (14)$$

Various disciplines, such as mathematics, science, and engineering, extensively utilize the Lambert  $W$  function. The Lambert  $W$  function is highly valuable for resolving transcendental equations and addressing exponential growth and decay problems that are not readily solvable using conventional functions. The Lambert  $W$  function enables the expression of equations containing exponential terms into more straightforward forms with analytical solutions. One frequently employed method involves utilizing an equivalence relationship to convert exponential equations into solvable forms by employing the Lambert  $W$  function. This allows for the discovery of manageable solutions to numerous intricate exponential equations that would otherwise lack a straightforward algebraic solution. [21–25]:

$$X = Ye^Y \Leftrightarrow Y = W(X) \quad (15)$$

By linking the expressions of the parameters to be extracted, substituting them in Equation (11), and applying Equation (15), the following equation can be derived:

$$\frac{I_{mp}R_s - V_{mp}}{nV_T} + \frac{V_{mp}I_{sc} - V_{oc}I_{mp}}{V_{mp}I_{sc} + V_{oc}(I_{mp} - I_{sc})} = W_{-1} \left( \exp \left( \frac{-\frac{V_{mp}I_{sc} - V_{oc}I_{mp}}{V_{mp}(2I_{mp} - I_{sc})}}{\frac{V_{mp}I_{sc} + V_{oc}(I_{mp} - I_{sc})}{2V_{mp} - V_{oc}}} \right) \right)$$

(16)

By using Equation (16), we can derive the explicit expression for the series resistance in the equivalent circuit [7], [25].

$$R_s = \frac{nV_T}{I_{mp}} W_{-1} \left( \frac{-\frac{V_{mp}(2I_{mp} - I_{sc})}{(V_{mp}I_{sc} + V_{oc}(I_{mp} - I_{sc}))}}{\exp\left(-\frac{V_{mp} - V_{oc}}{nV_T}\right)} \right)$$

(17)

Equations (17), (12), (9), and (8) allow for the calculation of the four parameters ( $R_s$ ,  $R_{sh}$ ,  $I_0$ , and

$I_{ph}$ ), respectively. This procedure determines the saturation current by calculating the ideality factor ( $n$ ), which is a dimensionless number ranging from 1 to 1.6.

The ideality factor quantifies the degree to which the diode conforms to the ideal diode equation. The presence of the ideality factor enables the computation of the saturation current. A diode that has an ideality factor closer to 1 exhibits a higher degree of adherence to the ideal equation. The knowledge of the ideality factor allows for the determination of the saturation current.

## 5. ANALYSIS AND DISCUSSION OF THE RESULTS

Table 2 clearly displays that the photocurrent ( $I_{ph}$ ) is always equal to the short-circuit current ( $I_{sc}$ ), even when the ideality factor ( $n$ ) changes.

This phenomenon arises due to the fact that the series resistance ( $R_s$ ) exhibits a significantly lower value compared to the shunt resistance ( $R_{sh}$ ) in these experimental scenarios. The results of this study show that the ideality factor doesn't change the fact that photocurrent and short-circuit current are the same, as long as the series resistance is much lower than the shunt resistance.

Because of the low value of  $R_s$  compared to  $R_{sh}$ ,  $I_{ph}$  equals  $I_{sc}$  for all estimated values of  $n$ .

This study emphasizes significant discrepancies in the values of series resistance ( $R_s$ ) and shunt resistance ( $R_{sh}$ ) that correspond to different ideality factors. The ideality factor demonstrates a clear contrast between its lowest value ( $n = 1$ ) and its highest value ( $n = 1.6$ ). The data highlights the significant impact of the ideality factor on the electrical properties of the system. When the ideality factor decreases to 1, both the series resistance ( $R_s$ ) and the shunt resistance ( $R_{sh}$ ) display noticeable variations, highlighting the system's susceptibility to changes in the ideality factor. On the other hand, an ideality factor of 1.6 results in different electrical characteristics, highlighting the significant influence of this factor on the performance of the system.

Table 2. Extracted parameters for estimated ideal factors ( $I_{ph}=I_{sc}$ )

n	$R_s(\Omega)$	$R_{sh}(\Omega)$	$I_0(A)$
1	0,3095	95,93	1,75E-08
1,1	0,2673	110,84	1,03E-07
1,2	0,2327	131,74	4,51E-07
1,3	0,1903	160,8	1,57E-06
1,4	0,1559	207,94	4,61E-06
1,5	0,1198	292,44	1,17E-05
1,6	0,0869	496,14	2,64E-05

As the ideality factor ( $n$ ) changes, Figures 6, 7, and 8 show how the series resistance ( $R_s$ ), shunt resistance ( $R_{sh}$ ), and saturation current ( $I_0$ ) change

Table 3. Parameter values of one PV cell

n	R <sub>s</sub> cell *1000(Ω)	R <sub>sh</sub> cell(Ω)
1	8,59	2,66
1.1	7,42	3,07
1.2	6,46	3,66
1.3	5,28	4,47
1.4	4,33	5,78
1.5	3,32	8,12
1.6	2,41	13,78

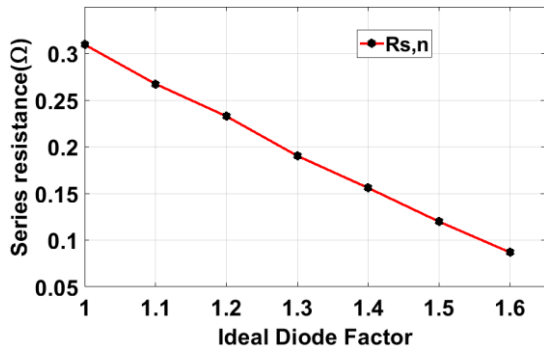


Fig. 6. Variations in the series resistance (Rs)

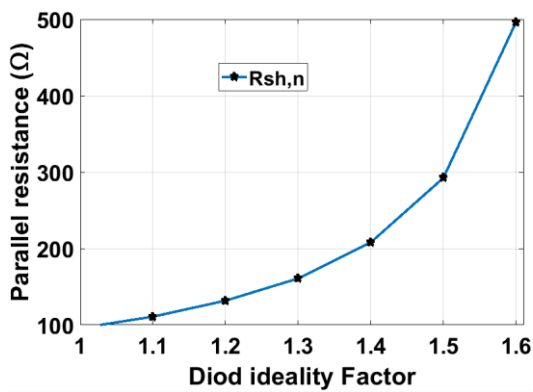


Fig. 7. Differences in branch resistance (Rsh)

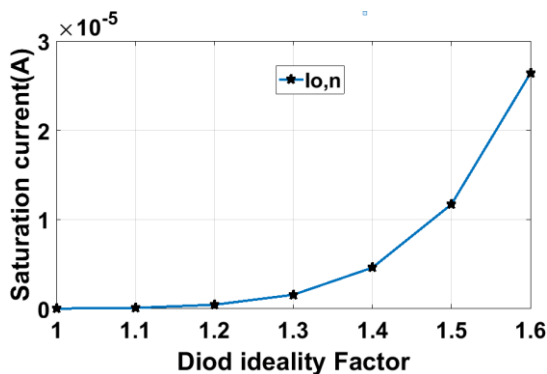


Fig. 8. The variation in the saturation current  $I_0$

The next step is to pick the best value for the diode ideality factor from the seven previous estimates. To do this, we use the serial and shunt resistance variation curves (Figures 6 and 8) to find the coordinates of this point on the graph. Here are the steps we take: To find the resistance values per cell, we divide the serial and shunt resistance values by the number of cells in the panel being studied (N

= 36). It's important to note that the serial resistance values are very small compared to the shunt resistance values, so we multiply Rs by 1000 as shown in Table 3 to make them the same order of magnitude.

Lastly, we graph the resistance curves for a solitary cell on a shared plot. We plot the curve of the series resistance (Rshcell multiplied by 1000) against the ideality factor (n), and we also plot the curve of the parallel resistance (Rscell) against the ideality factor. It is crucial to acknowledge that every curve possesses its own unique form. The Rscell curve exhibits a negative correlation with the ideality factor, whereas the Rshcell\*1000 curve demonstrates a positive correlation with an increase in the ideality factor.

The objective is to ascertain the coordinates of the points where these curves intersect. The points correspond to the state of equilibrium of the cell at a particular ideality factor. Put simply, the series and parallel resistances of the cell are equal at the intersection points. Analyzing the graph presented in Figure 9 accurately determines the precise value of the ideality factor.

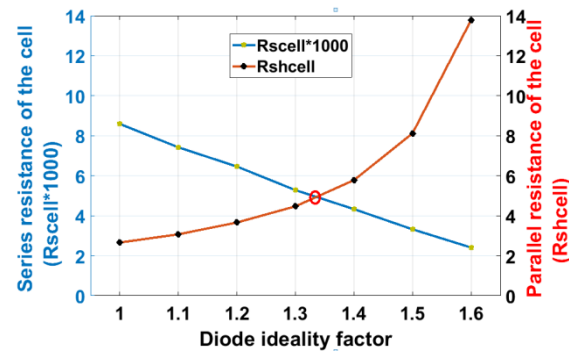


Fig. 9. Intersection of curves (1000\*Rscell and Rshcell) and determine the exact value of the ideal factor n graphically

Figure 9 determines the optimal zone as the area where the two curves intersect, indicating an ideality factor of n = 1.3. The precise point of intersection represents the optimal point, which produces the optimal value for n based on its x-coordinate. In order to accurately estimate the parameter values, we need to determine the exact value of the ideality factor. To achieve this, we narrow down the range of n to 1.3–1.35. Subsequently, we ascertain the resistor values for both series and parallel configurations that correspond to each specific ideality factor value. Using the Matlab software, Figure 10 displays the coordinates at which the curves Rscell \*1000 and Rshcell intersect.

It is crucial to emphasize that when we graphically determine the resistance value for the series configuration, we must divide the outcome by 1000 to obtain its accurate, initial value. By referring to Figure 10, we can use the available data to determine the exact coordinates of the intersection point.

$$X = n = 1,336 \text{ and } Y = RR_{\text{shcell}} = R_{\text{scell}} * 100 = 4,941\Omega$$

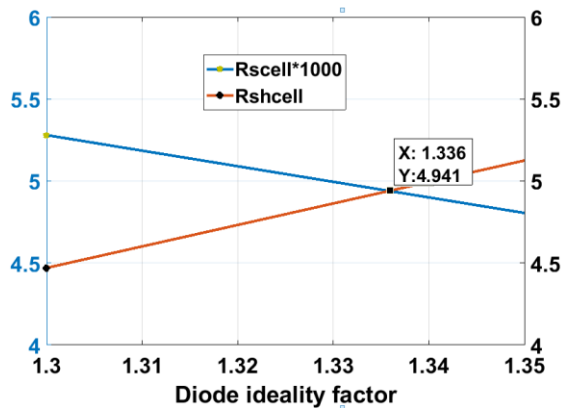


Fig.10. Spot where the Curve  $R_{\text{scell}} * 1000$  and the Curve  $R_{\text{shcell}}$  cross

Graphically inserting the parameter values of  $n$ ,  $R_{\text{scell}}$ , and  $R_{\text{shcell}}$  into equations (8) and (9) computes the values of  $I_0$  and  $I_{\text{ph}}$ . The resulting values are:  $I_0 = 3.158\text{E-}8$  A, and  $I_{\text{ph}} = 5.005\text{A}$ .

## 6. CONCLUSION

The main aim of this research paper is to streamline the process of retrieving internal data from solar cells. The process showcases the extraction of the five parameters ( $R_s$ ,  $R_{\text{sh}}$ ,  $I_0$ , and  $I_{\text{ph}}$ ) for the chosen equivalent circuit model by utilizing the manufacturer's datasheet. The Lambert-W function surpasses the inherent constraints of complex equations. In the  $[1-1.6]$  domain, we have identified the ideal value of the ideality factor, which is contingent upon the presence of parasitic resistances. Ultimately, it stabilized within the interval of  $[1.3-1.35]$ . We have determined the precise estimated value of the ideality factor to be 1.33. The novel approach demonstrates favorable performance in terms of accuracy. Scientists and technicians can utilize these principles to improve the effectiveness of solar cells and evaluate their ability to convert energy. The correct application of these principles promotes the development of environmentally friendly technology and the preservation of resources, resulting in enhanced efficiency of solar cells and broader utilization.

**Source of funding:** *This research received no external funding.*

**Author contributions:** *research concept and design, M.B.; Collection and/or assembly of data, M.B., M.B.R., S.M.; Data analysis and interpretation, M.B.R. A.N.; Writing the article, M.B., S.M.; Critical revision of the article, M.B.R., A.N., M.M.; Final approval of the article, M.M.*

**Declaration of competing interest:** *The authors declare that they have no known competing financial interests or personal relationships that could have appeared to influence the work reported in this paper.*

## REFERENCES

- Rabczak S, Proszak-Miąsik D. Analysis of Energy Yields from Selected Types of Photovoltaic Panels. *Journal of Ecological Engineering* 2020; 21(1): 20–8. <https://doi.org/10.12911/22998993/113471>.
- Pena-Bello A, Junod R, Ballif C, Wyrsh N. Balancing DSO interests and PV system economics with alternative tariffs. *Energy Policy* 2023; 183: 113828. <https://doi.org/10.1016/j.enpol.2023.113828>.
- Dunne NA, Liu P, Elbarghthi AFA, Yang Y, Dvorak V, Wen C. Performance evaluation of a solar photovoltaic-thermal (PV/T) air collector system. *Energy Conversion and Management: X* 2023; 20: 100466. <https://doi.org/10.1016/j.ecmx.2023.100466>.
- Amer A, Attar H, As'ad S, Alsaqoor S, Colak I, Alahmer A, et al. Floating Photovoltaics: Assessing the Potential, Advantages, and Challenges of Harnessing Solar Energy on Water Bodies. *Journal of Ecological Engineering* 2023; 24(10): 324–39. <https://doi.org/10.12911/22998993/170917>.
- Rawa M, Calasan M, Abusorrah A, Alhussainy AA, Al-Turki Y, Ali ZM, et al. Single Diode Solar Cells—Improved Model and Exact Current–Voltage Analytical Solution Based on Lambert's W Function. *Sensors* 2022;22(11):4173. <https://doi.org/10.3390/s22114173>.
- Huang PH, Xiao W, Peng JCH, Kirtley JL. Comprehensive Parameterization of Solar Cell: Improved Accuracy With Simulation Efficiency. *IEEE Transactions on Industrial Electronics* 2016; 63(3): 1549–1560. <https://doi.org/10.1109/tie.2015.2498139>.
- Aichouba MEA, Rahli M. Solar cell parameters extraction optimization using Lambert function. *Przegląd Elektrotechniczny* 2019; 95(4). <https://doi.org/10.15199/48.2019.04.43>.
- Bouzidi M, Harrouz A, Mohammed T, Mansouri S. Short and open circuit faults study in the PV system inverter. *International Journal of Power Electronics and Drive Systems (IJPEDS)* 2021; 12(3): 1764–71. <https://doi.org/10.11591/ijpeds.v12.i3.pp1764-1771>.
- Szabo R, Gontean A. Photovoltaic cell and module I-V characteristic approximation using Bézier curves. *Applied Sciences* 2018; 8(5): 655. <https://doi.org/10.3390/app8050655>.
- Calasan M, Abdel Aleem SHE, Zobaa AF. A new approach for parameters estimation of double and triple diode models of photovoltaic cells based on iterative Lambert W function. *Solar Energy* 2021; 218: 392–412. <https://doi.org/10.1016/j.solener.2021.02.038>.
- Szabo R, Gontean A. Photovoltaic cell and module I-V characteristic approximation using Bézier curves. *Applied Sciences* 2018; 8(5): 655. <https://doi.org/10.3390/app8050655>.
- Zhang Z, Ma M, Wang H, Wang H, Ma W, Zhang X. A fault diagnosis method for photovoltaic module current mismatch based on numerical analysis and statistics. *Solar Energy* 2021; 225: 221–36. <https://doi.org/10.1016/j.solener.2021.07.037>.
- Lee WC, Hwang DH. Improved SSJ-MPPT method for maximum power point tracking of photovoltaic inverter under partial shadow condition. *Journal of Electrical Engineering & Technology* 2019;14(1):

- 301–309. <https://doi.org/10.1007/s42835-018-00018-4>.
14. Rashad M, Żabnieńska-Góra A, Norman L, Jouhara H. Analysis of energy demand in a residential building using TRNSYS. *Energy* 2022; 254: 124357. <https://doi.org/10.1016/j.energy.2022.124357>.
  15. Mansoor M, Mirza AF, Ling Q. Harris hawk optimization-based MPPT control for PV systems under partial shading conditions. *Journal of Cleaner Production* 2020; 274: 122857. <https://doi.org/10.1016/j.jclepro.2020.122857>.
  16. Chaibi Y, Malvoni M, Chouder A, Boussetta M, Salhi M. Simple and efficient approach to detect and diagnose electrical faults and partial shading in photovoltaic systems. *Energy Conversion and Management* 2019; 196: 330–43. <https://doi.org/10.1016/j.enconman.2019.05.086>.
  17. Park JY, Choi SJ. A novel simulation model for PV panels based on datasheet parameter tuning. *Solar Energy* 2017; 145: 90–8. <https://doi.org/10.1016/j.solener.2016.12.003>.
  18. Rasool F, Drieberg M, Badruddin N, Mahinder Singh BS. PV panel modeling with improved parameter extraction technique. *Solar Energy* 2017; 153: 519–30. <https://doi.org/10.1016/j.solener.2017.05.078>.
  19. Sera D, Teodorescu R, Rodriguez P. PV panel model based on datasheet values. 2007 IEEE International Symposium on Industrial Electronics 2007 p. 2392–6. <https://doi.org/10.1109/ISIE.2007.4374981>.
  20. Calasan M, Nedic A. experimental testing and analytical solution by means of Lambert W-function of inductor air gap length. *Electric Power Components and Systems* 2018; 46(7): 852–862. <https://doi.org/10.1080/15325008.2018.1488012>.
  21. Calasan M, Abdel Aleem SHE, Zobaa AF. On the root mean square error (RMSE) calculation for parameter estimation of photovoltaic models: A novel exact analytical solution based on Lambert W function. *Energy Conversion and Management* 2020; 210: 112716. <https://doi.org/10.1016/j.enconman.2020.112716>.
  22. Mainardi F, Masina E, González-Santander JL. A Note on the Lambert W Function: Bernstein and stieltjes properties for a creep model in linear viscoelasticity. *Symmetry* 2023; 15(9): 1654. <https://doi.org/10.3390/sym15091654>.
  23. Wang J, Moniz NJ. Analysis of thermodynamic problems with the Lambert W function. *American Journal of Physics* 2019; 87(9): 752–7. <https://doi.org/10.1119/1.5115334>.
  24. Tayyan A. An approach to extract the parameters of solar cells from their illuminated I-V curves using the Lambert W function. *Turkish Journal of Physics* 2015; 39(1): 1–15. <https://doi.org/10.3906/fiz-1309-7>.
  25. Veberič D. Lambert W function for applications in physics. *Computer Physics Communications* 2012; 183(12): 2622–8. <https://doi.org/10.1016/j.cpc.2012.07.008>.
  26. Gaete MB, Gomez S, Hassaine M. Black holes with Lambert W function horizons. *The European Physical Journal C* 2019; 79(3): 200. <https://doi.org/10.1140/epjc/s10052-019-6723-6>.
  27. Racewicz S, Chrzan PJ, Riu DM, Retière NM. Time domain simulations of synchronous generator modelled by half-order system, IECON 2012, 2012:25–28. <https://ieeexplore.ieee.org/document/6388739>.
  28. Rawa M, Al-Turki Y, Sindi H, Calasan M, Ali ZM, Abdel Aleem SHE. Current-voltage curves of planar heterojunction perovskite solar cells – Novel expressions based on Lambert W function and Special Trans Function Theory. *Journal of Advanced Research* 2023; 44: 91–108. <https://doi.org/10.1016/j.jare.2022.03.017>.



#### Dr. BOUZIDI Mohammed

was born in Aoulef-Adrar, Algeria on 13/03/ 1981. He obtained his Master's degree in Electrical Engineering with a specialization in Control from the University of Béchar in 2015. Later, in 2023, He obtained a doctorate degree Electrical engineering specialty from the University of Adrar.

He is currently an associate professor at sciences and technology department, University of Tamanrasset. His research interests include fault detection in renewable energy systems using artificial intelligence, as well as industrial electric machines and networks. He is also an author and contributor to numerous research articles.

e-mail: [mohbouzidi81@yahoo.fr](mailto:mohbouzidi81@yahoo.fr)



#### Dr Mohamed BENRAHMOUNE

was born on 23/10/1988 in Messaad, Algeria. He received his PhD degree on Maintenance in Industrial Instrumentation in 2017 from University of Djelfa, He is currently working as a lecturer at Tamanghasset university since 2018. He is author and co-author of many publications and conferences papers, His research interests include: fault diagnosis of industrial systems, Photovoltaic systems, Control systems and Artificial Intelligence.

e-mail: [m.benrahmoune@univ-tam.dz](mailto:m.benrahmoune@univ-tam.dz)



#### Pr. Abdulfatah NASSRI

was born in 1978 in Bechar, Algeria. He is a full professor in the Department of Electrical Engineering at the Faculty of Science and Technology, University of Bechar - Algeria. He is considered an active member in the laboratory Smart Grid and Renewable Energy SGRE University Tahri Mohamed Bechar Algeria and is

an author and co-author of numerous published research papers in the fields of smart grids and renewable energy.

e-mail: [nasri.abdelfatah@univ-bechar.dz](mailto:nasri.abdelfatah@univ-bechar.dz)

**Dr MANSOURI Smail**

Was born on 10/05/1971 in Reggan, Adrar Algeria. Received his PhD degree On electrical engineering in 2017 from university of becher, he is currently an associate professor at Hydrocarbon and renewables energies department, university of adrar. He is author and co-author of many publications and conference papers, his

research interests include: control of wind system, diagnostic of solar system connected to network and artificial Intelligence.

e-mail: [mansouri197105@univ-adrar.edu.dz](mailto:mansouri197105@univ-adrar.edu.dz)

**Pr. Messaoud HAMOUDA**

was born in Adrar Algeria on 25 November 1962. He is a graduate of the University USTO in Oran (Algerai) in 1992. From the same University , he received his MSc degree in electrotechnic (1997) and his PhD in electrotechnic (2007). He has been managing director for seven years of the Renewable Energy Research

Unit in Saharan Medium in Adrar Algeria. He is a Professor at the University of Adrar. Currently, he is a director of Laboratory of the sustainable Development and informatic (LDDI). He is a member of many scientific and industrial organizations. He has organized a significant number of conferences, meetings, and study days on a national and international leve .He is director of several doctoral courses. His research interests concern: the integration of renewable energies, HVDC systems, and the Electrical Dischargese, optimization of energy flows in microgrids.

e-mail: [mes.hamouda@univ-adrar.edu.dz](mailto:mes.hamouda@univ-adrar.edu.dz)